

Electronic Supplementary Information (ESI)

Structural organic battery cathodes comprised of organic redox active polymers, reduced graphene oxide, and aramid nanofibers

Oka, S.¹; Thakur, R. M.¹; Easley, A. E.²; Green, M. J.^{1,2}; Lutkenhaus, J. L.^{1,2,*}

¹Artie McFerrin Department of Chemical Engineering, Texas A&M University, College Station, TX, USA 77843

²Department of Materials Science & Engineering, Texas A&M University, College Station, TX, USA 77843

*Correspondence:

Jodie Lutkenhaus, Tel: +1(979)-845-2682; E-mail: jodie.lutkenhaus@tamu.edu

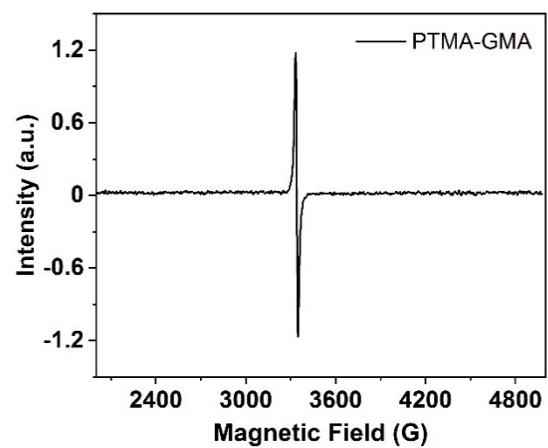


Figure S1: Electron paramagnetic resonance (EPR) spectra of PTMA-GMA

Table S1: Atomic weight percentages of nitrogen, carbon, and oxygen in 30 wt% PTMA-GMA, 50 wt% PTMA-GMA, and 70 wt% PTMA-GMA on rGO/BANF platform

	Nitrogen (at. %)	Carbon (at. %)	Oxygen (at. %)
30 wt% PTMA-GMA	2.6	66.3	31.1
50 wt% PTMA-GMA	3.3	61.2	35.5
70 wt% PTMA-GMA	3.7	60.4	35.9

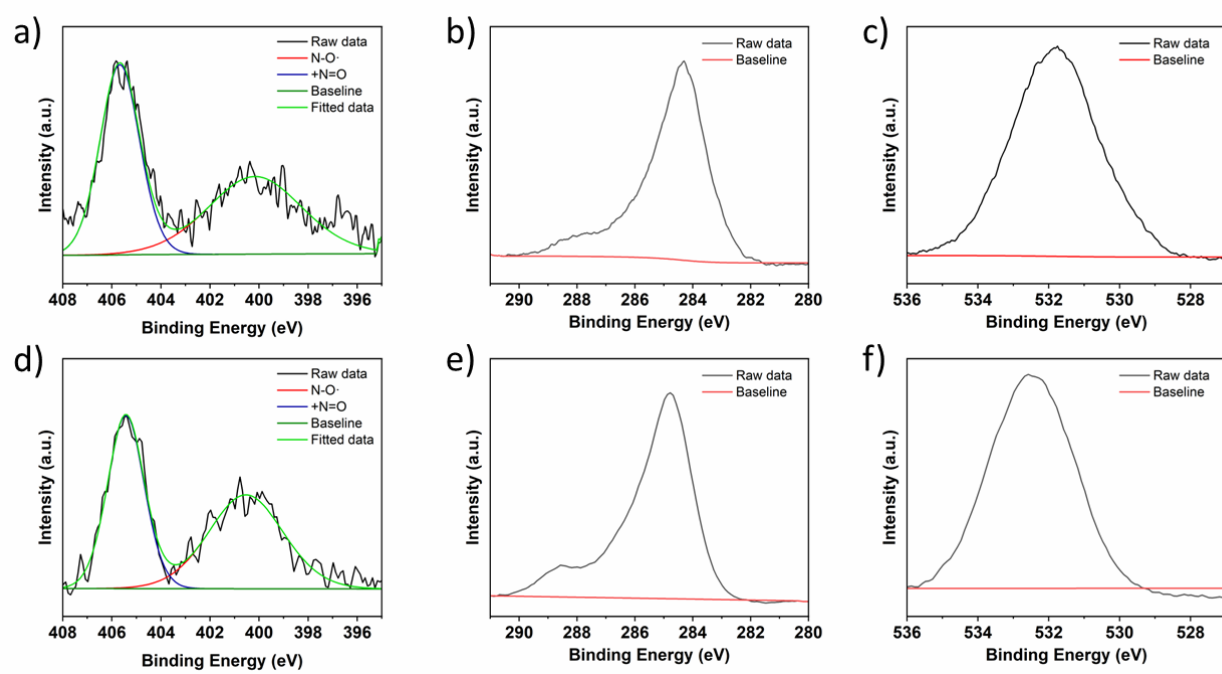


Figure S2: High-resolution XPS spectra for (a-c) 30 wt% PTMA-GMA on rGO/BANF with a) N 1s peak with deconvolution, b) C 1s peak, c) O 1s peak, and (d-f) 70 wt% PTMA-GMA on rGO/BANF with d) N 1s peak with deconvolution, e) C 1s peak, f) O 1s peak.

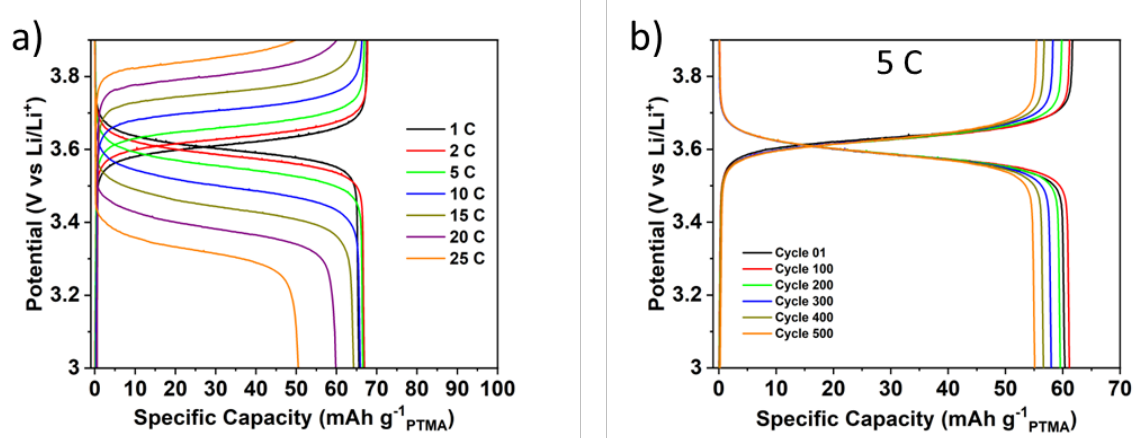


Figure S3: Galvanostatic charge-discharge (GCD) cycles for 50 wt% PTMA on rGO/BANF structural cathode during a) rate capability testing at different C-rates and b) long-term cycling 500 cycles at 5 C

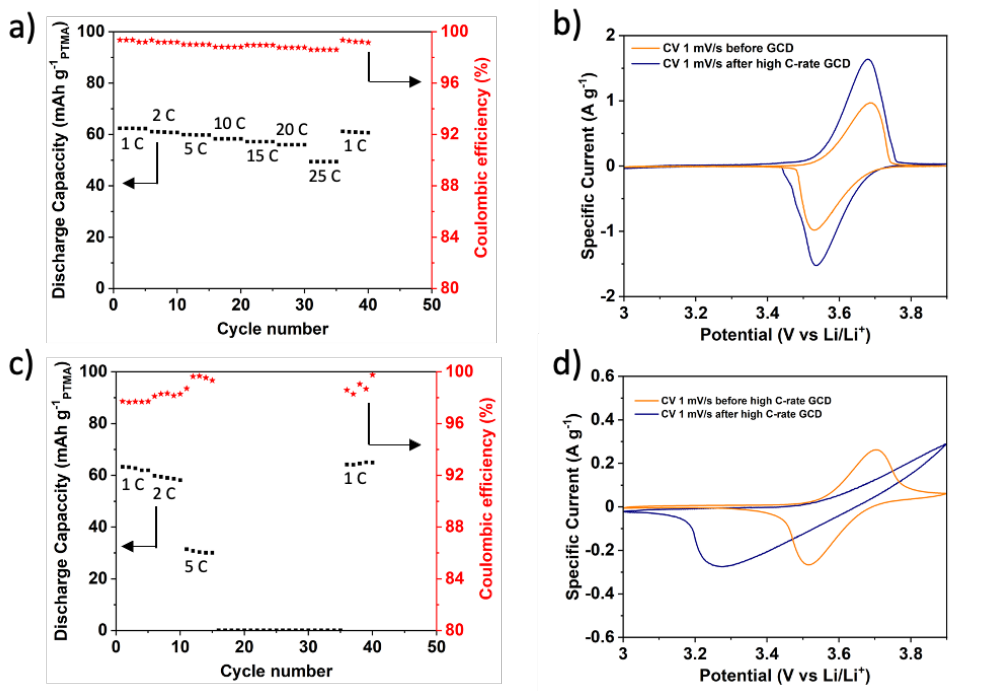


Figure S4: a) Rate capability GCD testing and b) CV before and after GCD testing of 30 wt% PTMA-GMA on rGO/BANF; c) rate capability GCD testing and d) CV before and after GCD testing of 70 wt% PTMA-GMA on rGO/BANF

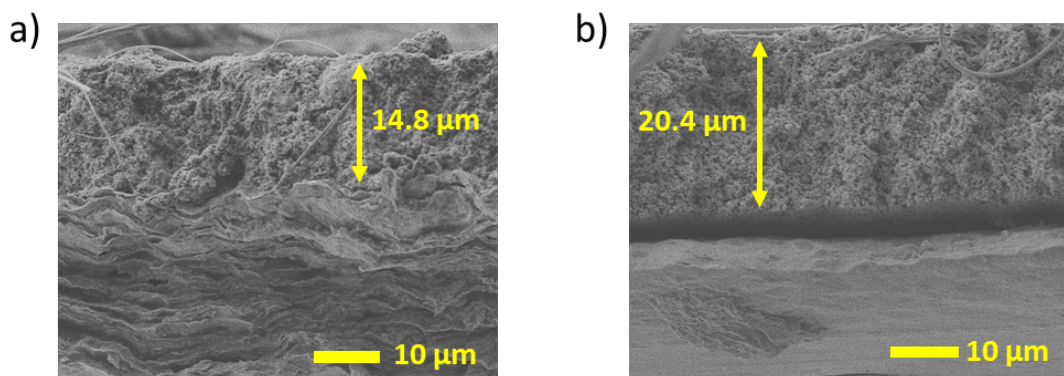


Figure S5: Cross-sectional scanning electron microscopy images of 50 wt% PTMA-GMA coated on a) rGO/BANF and b) aluminum foil after long-term GCD cycling

Table S2: Comparison of active material mass loading, specific energy, modulus, and power for PTMA-GMA on rGO/BANF electrodes from this work with commercial and other structural energy storage and organic battery electrode systems

Index	Material	Specific Capacity (mAh g ⁻¹) (at lowest C-rate tested)	Specific Energy (Wh kg ⁻¹) (at lowest C-rate tested)	Specific Modulus (GPa.cm ³ g ⁻¹)	Specific Power (W kg ⁻¹) (at highest C-rate tested)	Active material areal mass loading (mg/cm ²)	Highest C-rate tested
A	PTMA-GMA on rGO/BANF (this work)	66 (1 C)	231.1	4.33	4312.5	0.9 – 1.0	25 C
B	CF-based Li-S battery ¹	1200 (0.1 C)	2549.8	15	510	1.0	1 C
C	rGO/BANF/LFP ²	158 (0.3 C)	495	7.1	990	1.5	6 C
D	Commercial LFP ³	150 (0.1 C)	493	0.02	680	14.5	5 C
E	Commercial NCM ⁴	160 (0.2 C)	1097	0.99	548	6.3	5 C
F	Commercial graphite ⁵	330 (0.1 C)	140	0.7	432	6.5	5 C
G	CF/LFP/SB E pouch cell ⁶	30 (0.05 C)	90.1	9.9	34.7	8.2	3 C
H	CF/LCO ⁷	90 (0.1 C)	35	0.58	35	0.4	1 C
I	Coextruded CFRP composite ⁸	-	24	0.45	49.1	1.8	1 C
J	CF/LFP ⁹	116 (0.1 C)	360	6.6	12	-	1 C
K	PTAm/SWCNTs ¹⁰	80 (10 C)	330	0.01	2.05x10 ₅	16	620 C
L	PTMA/pyrene/rGO ¹¹	100 (1 C)	390	-	3600	0.6 - 0.8	20 C

M	PTMA ¹²	77 (0.1 C)	270	-	2415	1.1	10 C
N	PTVE ¹³	114 (0.6 C)	400	-	240	1.2	0.6 C
O	Melt-polymerized TEMPO methacrylate ¹⁴	90 (1 C)	315	-	4200	1	120 C
P	PTMA-co-GMA	104 (0.1 C)	364	-	525	-	10 C

References

1. W. Huang, P. Wang, X. Liao, Y. Chen, J. Borovilas, T. Jin, A. Li, Q. Cheng, Y. Zhang, H. Zhai, A. Chitu, Z. Shan and Y. Yang, *Energy Storage Materials*, 2020, **33**, 416-422.
2. P. Flouda, S. Oka, D. Loufakis, D. C. Lagoudas and J. L. Lutkenhaus, *ACS Applied Materials & Interfaces*, 2021, **13**, 34807-34817.
3. J. Lu, W. Li, C. Shen, D. Tang, L. Dai, G. Diao and M. Chen, *Ionics*, 2019, **25**, 4075-4082.
4. H. Zhong, M. Sun, Y. Li, J. He, J. Yang and L. Zhang, *Journal of Solid State Electrochemistry*, 2016, **20**, 1-8.
5. H. Zheng, L. Zhang, G. Liu, X. Song and V. S. Battaglia, *Journal of Power Sources*, 2012, **217**, 530-537.
6. L. E. Asp, K. Bouton, D. Carlstedt, S. Duan, R. Harnden, W. Johannisson, M. Johansen, M. K. G. Johansson, G. Lindbergh, F. Liu, K. Peuvot, L. M. Schneider, J. Xu and D. Zenkert, *Advanced Energy and Sustainability Research*, 2021, **2**, 2000093.
7. P. Liu, E. Sherman and A. Jacobsen, *Journal of Power Sources*, 2009, **189**, 646-650.
8. A. Thakur and X. Dong, *Manufacturing Letters*, 2020, **24**, 1-5.
9. K. Moyer, C. Meng, B. Marshall, O. Assal, J. Eaves, D. Perez, R. Karkkainen, L. Roberson and C. L. Pint, *Energy Storage Materials*, 2020, **24**, 676-681.
10. K. Hatakeyama-Sato, H. Wakamatsu, R. Katagiri, K. Oyaizu and H. Nishide, *Advanced Materials*, 2018, **30**, 1800900.
11. K. Zhang, Y. Hu, L. Wang, M. J. Monteiro and Z. Jia, *ACS Applied Materials & Interfaces*, 2017, **9**, 34900-34908.
12. K. Nakahara, S. Iwasa, M. Satoh, Y. Morioka, J. Iriyama, M. Suguro and E. Hasegawa, *Chemical Physics Letters*, 2002, **359**, 351-354.
13. M. Suguro, S. Iwasa, Y. Kusachi, Y. Morioka and K. Nakahara, *Macromolecular Rapid Communications*, 2007, **28**, 1929-1933.
14. A. Vlad, J. Rolland, G. Hauffman, B. Ernould and J.-F. Gohy, *ChemSusChem*, 2015, **8**, 1692-1696.